

Shaking Table Tests of Bridge Models with Friction Slip Dampers

Takeda, Atsushi

Technical Research Institute of Obayashi co.



SUMMARY:

Although introduction of vibration control systems for bridges have advantages in terms of both seismic performance and construction cost, seismic design method of the bridges utilizing dampers is still developing. The purpose of this study is to promote the design method of bridges utilizing dampers. This paper describes the result of shaking table tests of bridge models with friction slip dampers. Followings are found. (1) The dampers and the pier models exhibiting nonlinear behaviour resist to the earthquake action in cooperation. (2) The friction slip damper is effective to reduce the response displacement. (3) The contribution of the damper to the each level earthquake is determined.

Keywords: friction slip damper, shaking table test, vibration control, seismic design

1. INTRODUCTION

In addition to earthquake-resistant structures and seismic isolated structures, seismic response controlled structures have been attracting attention in recent years. Earthquake-resistant structures use the performance of the structural elements themselves to resist an earthquake. Seismic isolated structures reduce response to ground motion by making natural period long. On the other hand, in seismic response controlled structures, dampers absorb energy to reduce response. Adopting an seismic response controlled structure makes it possible to downsize member sections and reduce relative displacements (Amano et al 2010). But the seismic design method of bridges installing dampers is still developing.

On such background, the shaking table tests were carried out to promote the design method of bridges utilizing dampers. Followings are characteristics of the tests:

- (1) The tests are intended for use on bridge systems, and horizontal forces are born by piers and dampers in cooperation.
- (2) The friction slip dampers are used as the devices absorbing energy.
- (3) The tested bridge piers are RC structures and those responses includes non-linear areas.

The effects of the dampers and the dynamic behaviour of the bridge system with dampers installed were considered from the tests results compared with the case with no damper installation.

2. FRICTION SLIP DAMPERS

2.1. Summary of the Friction Slip Dampers

Figure 2.1. shows the basic configuration of the friction slip dampers used in this study (referred to below as “disc springs bolt unit”). The friction pad fastened to steel plates A and the stainless steel plates fastened to steel plate B slide over each other, generating frictional heat, and vibration energy is converted into heat energy. The normal force on the friction surfaces is generated by fastening high-tension bolts. The normal force is stabilized by disc springs. Steel plate B and its stainless steel plate are provided with slotted holes to avoid immobilizing the high-strength bolts. The friction pad

uses phenolic resin of high durability. If necessary, the number of friction surfaces can be increased, as shown in **Figure 2.2**.

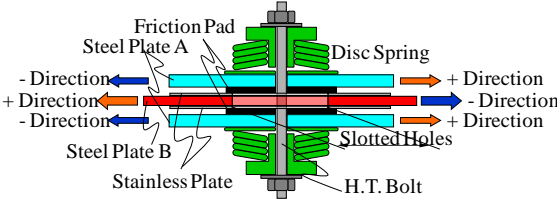


Figure 2.1. Disc springs bolt unit

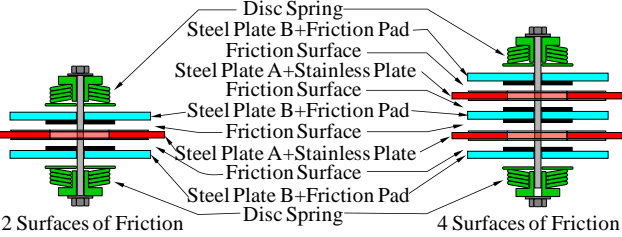


Figure 2.2. Increasing of friction surfaces

This damper has already been widely used in building structures(Sano, Suzui & Kanzaka 2003), then its use in bridges is also being considered, because of its low cost and the ease of lengthening its stroke(Amano et al 2010).

2.2. The Friction Slip Damper Used in This Test

Figure 2.3. shows the friction slip damper used in this test. There are two disc springs bolt units and two friction surfaces, and the bolt fastening force is 18.5 kN. A H-shaped steel is used for the steel plate A shown in **Figure 2.2**, and steel channels are used for the steel plate B shown in **Figure 2.2**. Damping capacity is calculated to be 25.9kN as the product of the friction factor (taking μ as 0.35), the bolt fastening force, number of disc springs bolt units, and number of friction surfaces.

For the tests, two of the same dampers are used in parallel, so they are called Damper No.1 and Damper No.2.

Before the shaking table tests, the performance tests of the dampers were carried out. The performance tests were performed with forced input of a dynamic sinusoidal displacement. The two dampers were also arranged in parallel in the performance tests, so their displacements were equal, and load cells were connected to them to measure the load on each damper. **Table 2.1.** shows the input wave for the performance test. The load pattern was configured as three waves at the target amplitude and two waves added on each side, increasing and then decreasing.

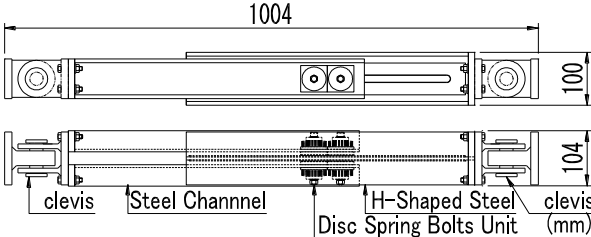


Figure 2.3. Damper used in the test

Table 2.1. Input motion of performance

tests No.	Waveform	Frequency (Hz)	Amplitude (mm)	Max Velocity (kine)	Wave Number
A-1	Sine Wave	0.25	100	15.7	3
A-2	Sine Wave	1.00	100	62.8	3
A-3	Sine Wave	2.00	100	125.7	3

Figure 2.4. shows the damping force - displacement relationship for the dampers, as obtained in the

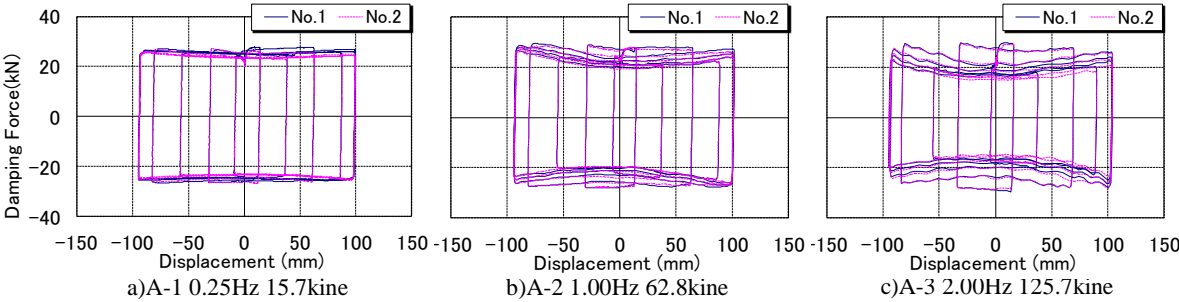


Figure 2.4. Damping force - displacement relationship of the damper

performance test. The shape of hysteresis loops of the damping force - displacement relationship is close to rectangular when maximum velocity is low, but can be seen to become increasingly concave on the top and bottom sides as maximum velocity increases. This velocity dependency is caused by the changing condition of the phenolic resin used for the friction pads with heating caused by friction, which is a property of the material.

3. TESTS METHOD

3.1. Summary of the Tests

Figure 3.1. shows setup of the tests. Two sets, each of one RC bridge pier model, one steel bridge abutment model, and one beam model, are placed on the shaking table. Only the front set in the photograph is equipped with friction slip dampers. Thus, the with-damper and without-damper cases are performed at the same time. The joint between the bridge pier model and the beam model is a clevis joint, forming a pin bearing which only transmits vertical and horizontal forces. The joint between the abutment model and the beam model uses a clevis joint and a linear guide, forming a pin roller bearing which only transmits vertical force. The friction slip dampers are used with two in parallel, as in the performance test, and there is a clevis on both ends of the damper between the beam model and the abutment model, so that only horizontal force is transmitted. The abutment model was assumed to be a rigid body, and was made 50 times as rigid as the bridge pier. Shaking was unidirectional (in the direction of longitudinal).

In this test, the details of the prototype were not determined, but a bridge with dampers between the abutment and the beam end was assumed, as shown in **Figure 3.2.** as an example. This bridge can be regarded as a one-mass model, as shown in **Figure 3.3.**, and the behaviour of multiple bridge piers can be aggregated in the bridge pier spring. Furthermore, considering that the total behaviour can be broadly expressed in a bilinear form, three parameters are required to define the vibration characteristics of this one-mass model: the natural frequency of the bridge system, which does not consider the dampers, the yield seismic intensity of the bridge pier, and the ratio between the yield strength of the damper spring and the superstructure weight (referred to below as “damper seismic intensity”). To determine these three parameters, the behaviour of the mass is defined uniquely. In this test, the parameters for the vibration characteristics of the prototype were assumed as follows, natural frequency (depending on secant stiffness on yielding): 1.0Hz, yield seismic intensity of the bridge pier: 0.38, damper seismic intensity: 0.1.

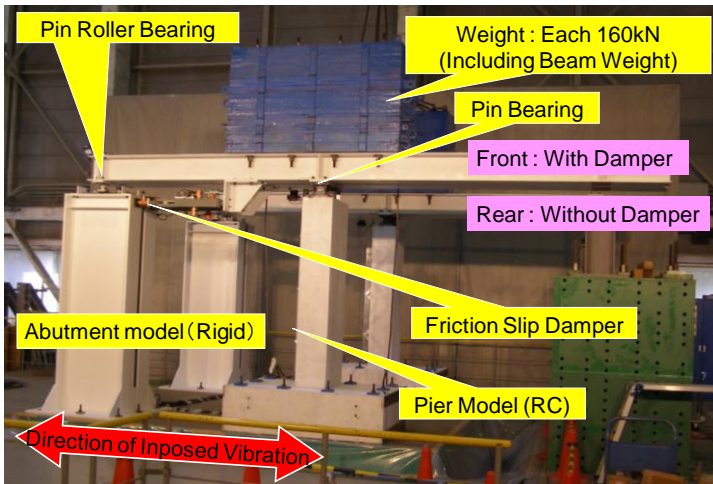


Figure 3.1. Set up of the tests



Figure 3.2. Example of assumed bridge

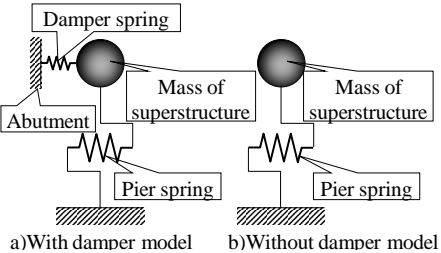


Figure 3.3. One mass model

3.2. Similarity rule

In this test, the dimensions of the prototype bridge are not determined, so it is possible to regard any size as actual size, and the similarity rule is not necessarily required. However, if the test specimen is determined by the performance limits of the shaking table, the dimensions of the bridge pier model become very small, so its behaviour as RC is unreliable. Considering the purpose of this test, the behaviour of the plastic hinge is extremely important, so we decided to define the similarity rule.

The similarity rule was set so that velocity would be equal with the prototype. This is because, as describe in section 2.2., the velocity dependency of the friction slip damper is very strong. Also, based on the vibration performance of the shaking table, the homothetic ratio for horizontal acceleration $1/\beta$ (A_m/A_p , where A_m and A_p are the accelerations in the test and in the prototype, respectively) was set to 3.0, and the superstructure weight (the total of the weight and beam) was set to 160 kN. **Table 3.1.** summarizes the homothetic ratios obtained as a result.

3.3. Bridge pier models

The bridge pier models were designed so that the natural frequency derived from the secant stiffness at initial yielding and the yield seismic intensity are the same as the values described in section 3.1. **Figure 3.4.** shows the reinforcement arrangement of the bridge pier model. There was no difference between the bridge pier model for the case with dampers and the one for the case without.

Table 3.1. Similarity rule

	Symbol	Homothetic Ratio	Prototype	Test
Horizontal Displacement	β	0.33		
Horizontal Velocity	1	1.00		
Horizontal Acceleration	$1/\beta$	3.00		
Time	β	0.33		
Natural Frequency(Hz)	$1/\beta$	3.00	1.00	3.00
Yieldinf Seismic Intensity	$1/\beta$	3.00	0.38	1.15
Damper Seismic Intensity	$1/\beta$	3.00	0.10	0.30

*Homothetic ratio is test scale / prototype scale

*Natural frequency depends on secant stiffness when yielding occurs

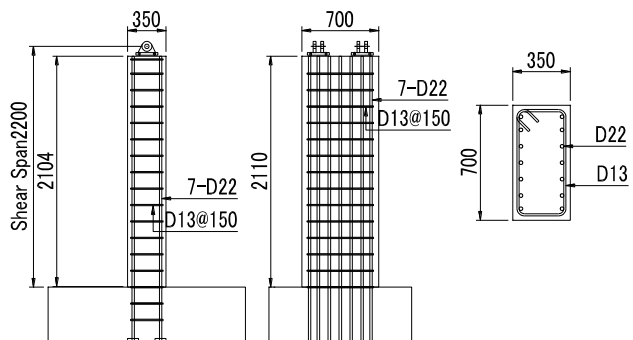


Figure 3.4. Bridge pier model

According to the FEA, the yield load of the bridge pier model was 183 kN, and the yield displacement was 31.6 mm. Therefore, the natural frequency derived from the secant stiffness on yielding is 3.00 Hz and the yield seismic intensity is 1.14, so the design is close to the targets.

Shear reinforcing bars were provided sufficiently to prevent shear failure, and the shear reinforcing bar ratio was 0.21%.

3.4. Input seismic waves

The input seismic waves used were Level 1 motion (referred as "L1"), Level 2 Type I motion (referred as "T-I") and Level 2 Type II motion (referred as "T-II"), as stated in the specifications for highway bridges (2002), adjusted by the similarity rule indicated in **Table 3.1.** **Figure 3.5.** shows the response spectra of the input seismic waves, **Table 3.2.** shows the details of the input seismic waves, and **Figure 3.6.** shows the waveforms of the input. Only one set of bridge pier models was used, and the shaking patterns 1~3, as shown in **Table 3.2.**, were applied sequentially to the same test specimen. Between these shaking patterns 1~3, shaking with a low multiplying factor was applied for the purpose of seismic wave adjustment. But this paper describes only 100% shaking as shown in **Table 3.2.**

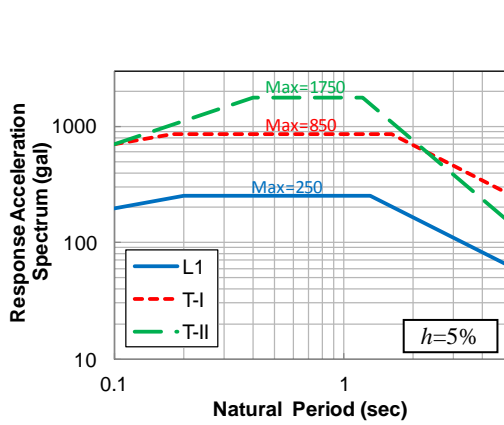
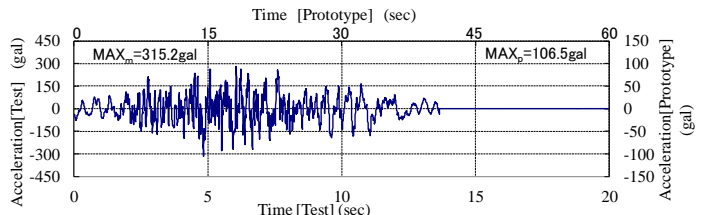
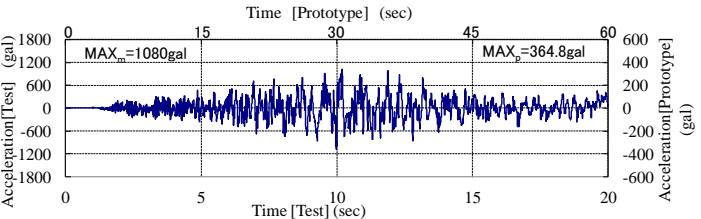


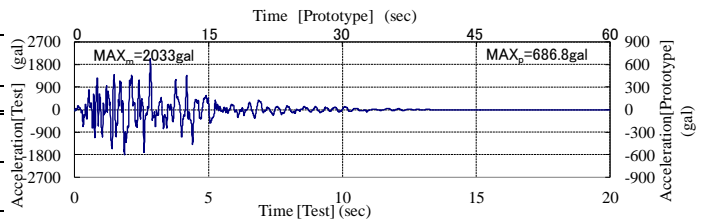
Figure 3.5. Response spectra of input motions



1) L1 motion



2) L2 T-I motion



3) L2 T-II motion

Figure 3.6. Wave forms of input motions

Table 3.2. Details of the input seismic waves

No.	Input motion	Grond Type	Phase Characteristics	Max. Acceleration (gal)	
				Prototype	Test
1	L1 Motion	II	1968 ITAJIMA BRG. LG.	106.5	315.2
2	L2(T-I) Motion	II	1994ONNETTO BRG. TR.	364.8	1079.8
3	L2(T-II) Motion	II	1995 JR TAKATORI STA. N-S	686.8	2032.9

4. TEST RESULTS

4.1. Response to L1 ground motion

Figure 4.1. shows the displacement time history of the top of the bridge pier under L1 ground motion. Figure 4.2. shows the load - displacement relationship, and Figure 4.3. shows the damping force - displacement relationship of dampers. The bridge pier top displacement was measured at the height

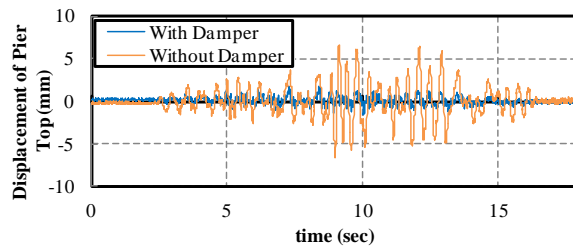


Figure 4.1. Waveform for displacement of the top of the bridge pier Bridge pier (L1)

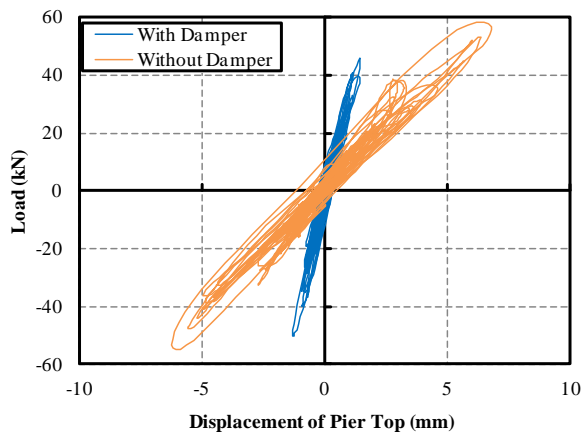


Figure 4.2. Load - displacement relationship

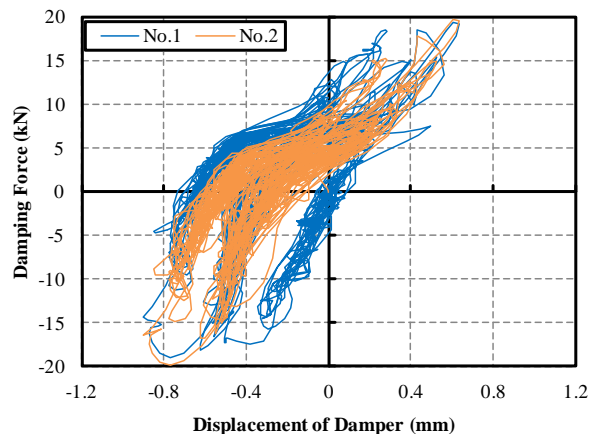


Figure 4.3. Damping force - displacement relationship of dampers (L1)

the pin center of the clevis that is the hinge bearing, using a laser displacement gauge. Load was calculated by multiplying the bridge pier top acceleration record by the mass of superstructure. Damping force of the dampers was measured using a load cells connected to the dampers. Damper displacement was measured relative displacement between the beam model and the abutment using a laser displacement gauge.

From **Figures 4.1.** and **4.2.**, it can be seen that the maximum response displacement without dampers was 6.66 mm, but that fell to 1.74 mm with dampers installed, a reduction to approximately 26%. However, from **Figure 4.3.**, it can be seen that the dampers had not reached maximum damping force at that time, and that there was almost no hysteretic damping. Therefore, it appears that this is due to differences in stiffness, and not to the damping effect of the dampers.

In each case, damage to the bridge pier was only cracking slightly by bending moment, and reinforcing bar strain did not reach yield.

Figure 4.3. shows that the two dampers showed mostly the same behaviour, indicating that there was little individual difference between the dampers.

4.2. Response to T-I and T-II ground motions

The displacement time history of the top of the bridge pier under inputs of T-I and T-II motions are shown in **Figures 4.4.** and **4.5.**, respectively. The load - displacement relationships are shown in **Figures 4.6.** and **4.7.**, and damping force - displacement relationships of dampers are shown in **Figures 4.8.** and **4.9.**

Maximum response displacements without dampers were 48.3 mm (T-I) and 145 mm (T-II), but installation of dampers changes those displacements to 16.1 mm (T-I) and 58.4 mm (T-II), reductions to approximately 33~40%. The main reason for the reduction appears to be that, as shown in **Figures 4.8.** and **4.9.**, there was major hysteretic damping in the dampers. However, the ratio of reduction is smaller than under L1 motion, due to the effect of stiffness.

In the case with dampers, the reinforcing bars did not reach yielding under T-I motion. Cracks were not widely open after the end of shaking, and were very slight. By T-II motion, the longitudinal reinforcements yielded at the base at around 5.1 seconds, roughly the same time as maximum displacement was reached in the case without dampers. Final residual strain in the base reinforcing bars was around 8,000 μ , and the damage was very similar to that of the case of T-I shaking without dampers.

In the case without dampers, the damage to the bridge pier model by T-I motion was yielding of the longitudinal bars in the base at around 12.1 seconds, residual strain of around 8,000 μ in the base longitudinal bars and diagonal cracking 1~2 mm wide. **Figures 4.10.** shows the base after the end of T- I motion. By T-II motion, maximum displacement (145 mm) was reached at around 5.1 seconds, and then immediately direction of displacement changed oppositely and buckling of compressive longitudinal bars to out-of-plane occurred. At that time, the cover concrete spalled off. **Figure 4.11.** shows the base after the end of T- II motion.

As shown in **Figures 4.8.** and **4.9.**, the damper behavior indicates a loop close to rectangular, indicating extraordinarily large energy absorption. Also, the two dampers showed mostly the same behavior, indicating that there was little individual difference between them. The maximum velocity in each shaking was 33.6 kine (T-I) and 103 kine (T-II), but compared to the hysteresis in **Figure 2.4.**, the concavity of the loop is clearly reduced. Therefore, if the performance of the dampers is assessed on the basis of its effect against a sine wave, hysteretic damping is assessed at a lower level, which would be on the safe side.

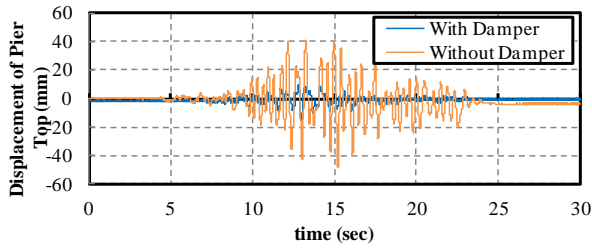


Figure 4.4. Waveform for displacement of the top of the bridge pier Bridge pier (T-I)

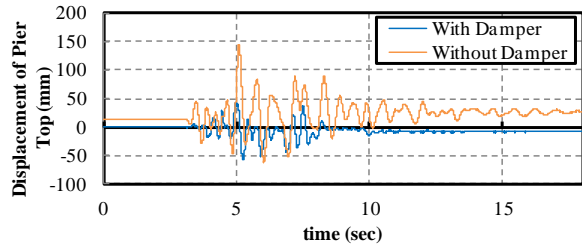


Figure 4.5. Waveform for displacement of the top of the bridge pier Bridge pier (T-II)

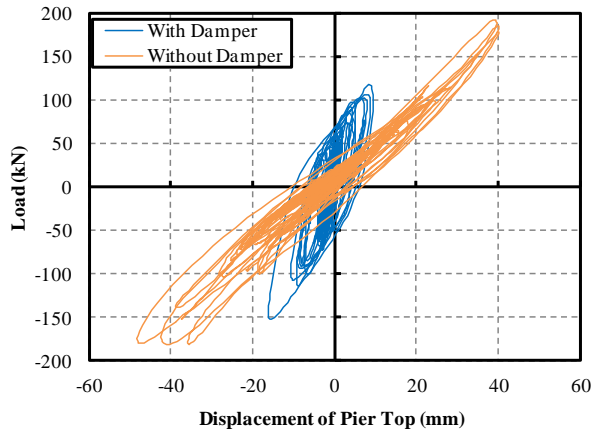


Figure 4.6. Load - displacement relationship (T-I)

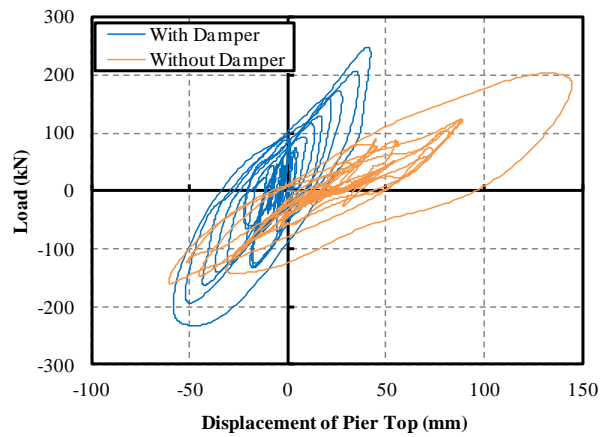


Figure 4.7. Load - displacement relationship

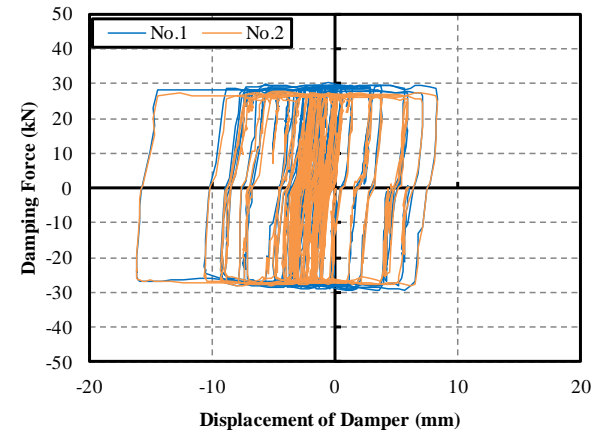


Figure 4.8. Damping force - displacement relationship of dampers (T-I)

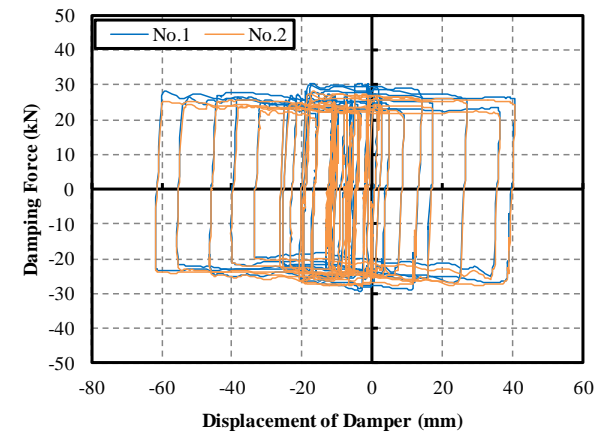


Figure 4.9. Damping force - displacement relationship of dampers (T-II)

Figures 4.12. and **4.13.** show the cumulative values of hysteretic energy absorption during the shaking of T-I and T-II motions, respectively. The hysteretic energy absorption of the bridge pier model can be considered as an indicator of the level of damage. Furthermore, the ultimate amount of hysteretic energy absorption is equal to the energy of the input waves with the viscous damping and radiation damping deducted.

The overall hysteretic energy absorption can be calculated as the integral values from the load - displacement relationships in **Figures 4.6.** and **4.7.**, while the hysteretic energy absorption in the dampers can be calculated as the integral values from the damping force - displacement relationships of dampers in **Figures 4.8.** and **4.9.**. The hysteretic energy absorption in the bridge pier in the case with dampers is calculated by subtracting the hysteretic energy absorption in the dampers from the total. The damper hysteretic energy absorption for T-I motion in the case with dampers cannot be read from the graph because it largely overlaps with the overall hysteretic energy absorption.

Comparing the response to T-I motion shown in **Figure 4.12.**, the overall hysteretic energy absorption in the case with dampers is smaller than in the case without dampers. This appears to be because the bridge pier model is in an elastic state, so the proportion from viscous damping etc. is higher. Even so, the hysteretic energy absorption is around 80% of that in the case without dampers, indicating that nearly all is received by the dampers. In other words, it is clear that the purpose of seismic response controlled structures, that the dampers absorb vibration energy and suppress damage to the bridge pier, is achieved.

Comparing the response to T-II motion shown in **Figure 4.13.**, the overall hysteretic energy absorption in the case with dampers is larger than in the case without dampers. This appears to be because there was major damage at around 5.1 seconds in the case without dampers, so the energy absorption performance of the bridge pier was reduced. It can be seen that the hysteretic energy absorbed by the dampers was around the same amount as that absorbed by the bridge pier in the case without dampers. As section 3.1 shows, the damper seismic intensity is around 1/4 of the yield seismic intensity of the bridge pier model, but as the hysteretic form is close to a rectangle, it provides major hysteretic damping.



Figure 4.10. Damage to bridge pier base by T-I motion without dampers



Figure 4.11. Damage to bridge pier base by T-II motion without dampers

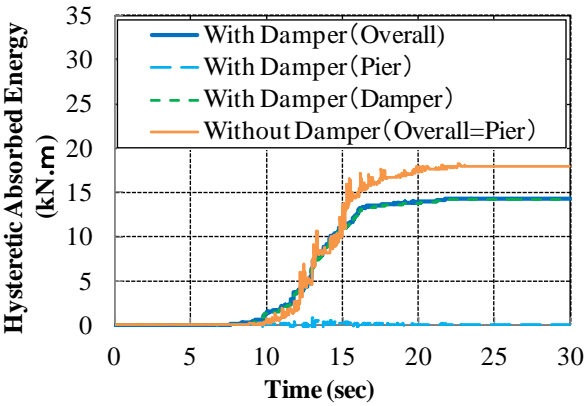


Figure 4.12. Hysteretic absorbed energy (T-I)

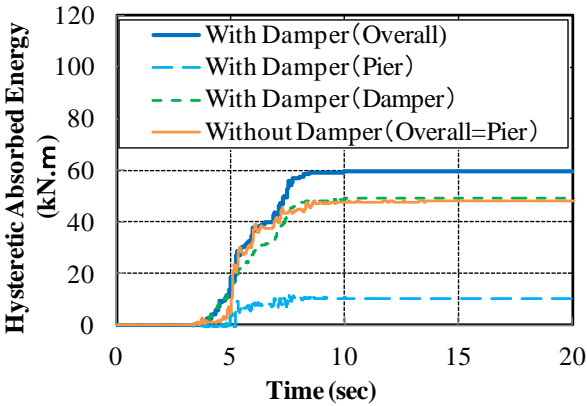


Figure 4.13. Hysteretic absorbed energy (T-II)

5. CONCLUSION

We performed shaking table tests on an entire bridge system with the aim of clarifying its behavior when the bridge is a seismic response controlled structure. For the shaking table tests, two sets, each consisting of one RC bridge pier model, one steel bridge abutment model, and one beam model, were placed on the shaking table, and only one set was equipped with friction slip dampers. In the structure, only the bridge pier model and the friction slip dampers resisted horizontal forces. The test results revealed the following:

- 1) The use of dampers was able to reduce response displacement under moderate-size earthquake as L1 motion. The effect of the dampers in that situation was due to increased stiffness in the system as a whole.
- 2) The use of dampers was able to reduce response displacement under huge earthquake as L2(T-I and T-II) motions. The effect of the dampers in that situation was mainly due to hysteretic damping. However, the proportion of reduction in response displacement was smaller than that under moderate-size earthquakes.
- 3) Even though the yield seismic intensity of the dampers was around 1/4 of that for the bridge pier, most of the vibration energy under huge earthquake was absorbed by the dampers.
- 4) The two friction slip dampers used in parallel in the test showed largely the same behavior, with little individual difference between them.

This study examined results of tests in one case, so it has not reached the level of a quantitative assessment. In the future, it will be necessary to construct a design method through further data collection and deeper study.

REFERENCES

- Amano, H., Ina, Y., Niihara, I. and Takeda, A. (2010). Applicability Study for Bridges with Friction Slip Dampers, *Proceedings of Annual Conference of the Japan Society of Civil Engineers*. **Vol.65**: 1141-1142.(in Japanese)
- Sano, T., Suzui, Y. And Kanzaka, Y. (2003). Introduction of the Brake Damper and an Applied Building Example. *Report of Obayashi Corporation Technical Research Institute*. **Vol.67**:No.37. (in Japanese)
- Japan Road Association. (2002). PartV Seismic Design, Specifications For Highway Bridges, Maruzen Company, Limited, Japan. (in Japanese)